Chemistry Letters Vol.37, No.12 (2008)

Anti-ferroelectric Banana Phase in a Bent-shaped Molecule with a Low Bend Angle of 60°

Seng Kue Lee,* Lu Shi, Ryohei Ishige, Sungmin Kang, Masatoshi Tokita, and Junji Watanabe
Department of Organic and Polymeric Materials, Tokyo Institute of Technology,
2-12-1 O-okayama, Meguro-ku, Tokyo 152-8552

(Received September 12, 2008; CL-080878; E-mail: sklee@polymer.titech.ac.jp)

This paper presents the first example of an antiferroelectric banana phase in a bent molecule with a low bend angle of about 60°.

Since the discovery of the spontaneous formation of polar-ordered superstructures and chiral symmetry breaking in bent-shaped (or banana) molecules, the unconventional mesomorphic properties of these molecules have opened up a highly innovative area in liquid crystal research, providing new science into the soft materials.[1–3] A number of bent-shaped molecules have been prepared and characterized, and at least eight different banana (B) phases have been identified.[4,5]

One of the major research targets in the banana liquid crystal field is to clarify how the molecular structure relates to mesophase properties such as polarity, chirality, and frustration. Though a variety of bent-shaped molecules have been synthesized, most of the central cores used are resorcinol derivatives with bent angles of about 120°. This bent angle is significant, as banana phases have been absent in bent-shaped molecules with lower and higher angles. Matsuzaki and Matsunaga have reported,[6] for example, that bent-shaped molecules based on 1,2-phenylene and 2,3-naphthylene groups, molecules with bent angles of about 60°, form only conventional nematic and smectic phases. This occurs simply because the molecules assume U-like shapes and behave like calamitic molecules rather than bent ones.

Watanabe et al.[7] recently prepared six bent-shaped molecules with classical side wings containing Schiff-base moieties at different positions of the central naphthalene core, in order to study and discuss the effects of the substituent position. Intriguingly, the derivative with the 1,7-naphthalene core forms a typical chiral B4 phase irrespective of its low bend angle of around 60°; however, no switchable banana phases have been found. In this study we prepared a homologous bent-shaped molecule with the same central naphthalene core and long side wings in which one phenyl ring is attached to the classic one via an ester linkage, as shown in Scheme 1.[17] As a result of the expanded mesophase temperature region, an antiferroelectric banana phase similar to the typical B2 phase was formed here in addition to the solid B4 phase.

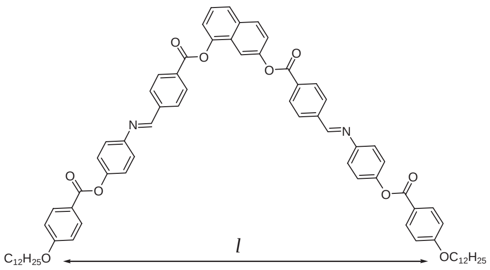

Scheme 1.

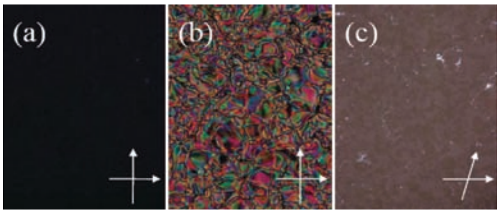

Figure 1. Photomicrographs for the (a) homeotropic smectic A, (b) non-tilted polar smectic A (SmAP$_A$), and (c) B4 phases. White arrows indicate the directions of polarity.

The transition behavior is as follows: isotropic (251.5 °C/$\Delta H = 0.31$ kJ mol^{-1})–nematic (N) (244.7 °C/$\Delta H = 0.59$ kJ mol^{-1})–smectic A (SmA) (240.1 °C/$\Delta H = 12.7$ kJ mol^{-1})–non-tilted polar smectic (SmAP$_A$) (205.6 °C/$\Delta H = 23.6$ kJ mol^{-1})–B4 upon decreasing temperature. The N phase was identified by the observation of a typical schlieren texture. On cooling from the nematic, the SmA phase appears with a black homeotropic texture (Figure 1a) and quickly transforms to the SmAP$_A$, which in turn shows a highly birefringent schlieren-like homeotropic texture (Figure 1b). The texture darkens with further cooling to the B4 phase, but with chiral segregation domains in which the brightness is interchanged by the positive and negative rotations of the polarizer from the cross polarization position (Figure 1c).

Though electric switching behavior is observed for the SmAP$_A$, no electrooptical measurements are possible for the higher-temperature SmA phase because of its very narrow temperature span. The application of a rectangular-wave field results in the development of fan-shaped domains, even when the sample in the cell is prepared with homeotropic alignment (Figure 2). This means that the polar direction is parallel to the layer. A birefringent color changes from red in the off-state to blue the on-state, whereas the extinction directions parallel and perpendicular to the layer remain unchanged in both the on- and off-states. Thus, the molecules lie perpendicular to the layer and the polar-

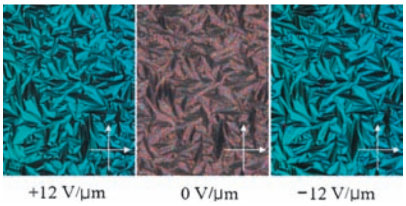

Figure 2. Photomicrographs illustrating the switching behavior in the SmAP$_A$ phase under an electric field. A sample of 5.0 μm in thickness was sandwiched between glass substrates with ITO electrodes.

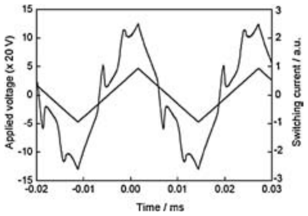

Figure 3. Polarization reversal current in the $SmAP_A$ phase at 220 °C under the application of a 180 V_{pp} triangular-wave voltage of 40 Hz. The cell observed was the same as that used for Figure 2.

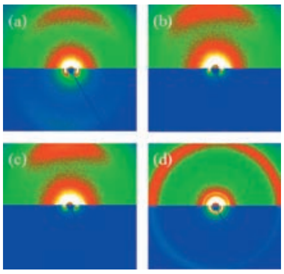

Figure 4. X-ray diffraction patterns for the (a) nematic, (b) smectic A, (c) nontilted polar smectic A ($SmAP_A$), and (d) B4 phases. The magnetic field is in a vertical direction.

ization reversal takes place by a rotation of the molecules around their long axis. Figure 3 shows the polarization reversal current peaks observed in a triangular-wave electric field. The double switching current peaks in the half cycle illustrate the antiferroelectric structure. The spontaneous polarization is about 500 nC/cm^2.

The X-ray diffraction measurement was performed under a magnetic field. The well-aligned sample was initially prepared for the N phase, and then X-ray patterns were observed on cooling (Figure 4). The N phase shows a pair of reflections: one inner diffuse reflection on the equator and one outer broad reflection on the meridian (Figure 4a). On entering the SmA and $SmAP_A$ phases, the inner reflection (the layer reflection) sharpens, whereas the outer broad reflection remains unchanged (Figures 4b and 4c). The layer spacings (42.3 Å) are almost the same for the SmA and $SmAP_A$ phases and correspond to the end-to-end distance (42.0 Å), as given by l in Scheme 1. Thus, the molecules are packed with the bent direction parallel to the layer and the molecular axis perpendicular to the layer in these smectic phases. The loss of the biaxiaity in SmA may be due to the short correlation length of polar packing.[8–10] Unlike the well-oriented X-ray patterns of the higher-temperature phases, the X-ray pattern of the B4 phase loses the orientation: all of the reflections appear as rings (Figure 4d). This apparent disorientation can be explained by the twist grain boundary-like helical structure.[11,12] The layer spacing of B4 phase is also 42.3 Å, suggesting that the molecular packing is not essentially changed from the two preceding phases.

Figure 5, a schematic illustration of the packing model for the notable $SmAP_A$ phase, is provided as a summary. $SmAP_A$ is a nontilted biaxial SmA phase with an antiferroelectric type of polarity (P_A), and electrooptical switching takes place between $SmAP_A$ and $SmAP_F$.[8–10] Note that the chiral segregation domain of the B4 phase is not memorized once the cell is heated up to the $SmAP_A$ phase.[13,14] This means that $SmAP_A$ is not chiral. This is the first example of a switchable banana phase in a low bend angle molecular system with a bent angle of about 60°. The unusual formation of the polar phase may be a consequence of the long distance between the positions of the two sticking side wings, as the gap may interrupt the molecular association into calamitic liquid crystals as U-shaped molecules.

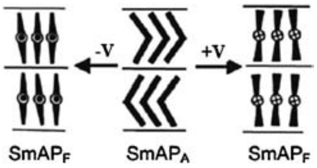

Figure 5. Schematic representation of the packing model for the $SmAP_A$ phase and polar switching to $SmAP_F$.

The ferroelectric and antiferroelectric switching of polar smectic phases can be applied to an in-plane switching display using a homeotropically aligned cell.[15,16] From this perspective, the high spontaneous polarization (500 nC/cm^2) and high birefringence due to the low bend angle endow this molecule with advantages over conventional banana molecules with a high bend angle. Thus, the present result opens up prospects for new, considerably extended molecular designs for bent-shaped molecules in both fundamental and applied fields.

References and Notes

1 T. Niori, T. Sekine, J. Watanabe, T. Furukawa, H. Takezoe, *J. Mater. Chem.* **1996**, *6*, 1231.
2 D. R. Link, G. Natale, R. Shao, J. E. Maclennan, N. A. Clark, E. Korblova, D. M. Walba, *Science* **1997**, *278*, 1924.
3 G. Pelzl, S. Diele, W. Weissflog, *Adv. Mater.* **1999**, *11*, 707.
4 H. Takezoe, Y. Takanishi, *Jpn. J. Appl. Phys.* **2006**, *45*, 597.
5 R. A. Reddy, C. Tschierske, *J. Mater. Chem.* **2006**, *16*, 907.
6 H. Matsuzaki, Y. Matsunaga, *Liq. Cryst.* **1993**, *14*, 105.
7 S. K. Lee, Y. Naito, L. Shi, M. Tokita, H. Takezoe, J. Watanabe, *Liq. Cryst.* **2007**, *34*, 935.
8 W. Weissflog, H. Nadasi, U. Dunemann, G. Pelzl, S. Diele, A. Eremin, H. Kresse, *J. Mater. Chem.* **2001**, *11*, 2748.
9 A. Eremin, S. Diele, G. Pelzl, H. Nadasi, W. Weissflog, J. Salfetnikova, H. Kresse, *Phys. Rev. E* **2001**, *64*, 051707.
10 R. A. Reddy, B. K. Sadashiva, *J. Mater. Chem.* **2004**, *14*, 310.
11 J. Thisayukta, Y. Nakayama, S. Kawauchi, H. Takezoe, J. Watanabe, *J. Am. Chem. Soc.* **2000**, *122*, 7441.
12 J. Thisayukta, H. Takezoe, J. Watanabe, *Jpn. J. Appl. Phys.* **2001**, *40*, 3277.
13 H. Niwano, M. Nakata, J. Thisayukta, D. R. Link, H. Takezoe, J. Watanabe, *J. Phys. Chem. B* **2004**, *108*, 14889.
14 S. K. Lee, L. Shi, M. Tokita, J. Watanabe, *J. Phys. Chem. B* **2008**, *112*, 6762.
15 D. Pociecha, M. Cepic, E. Gorecka, J. Mieczkowski, *Phys. Rev. Lett.* **2003**, *91*, 185501.
16 Y. Shimbo, Y. Takanishi, K. Ishikawa, E. Gorecka, D. Pociecha, J. Mieczkowski, K. Gomola, H. Takezoe, *Jpn. J. Appl. Phys.* **2006**, *45*, L282.
17 Supporting Information is also available electronically on the CSJ-Journal Web site, http://www.csj.jp/journals/chem-lett/index.html.

Published on the web (Advance View) November 1, 2008; doi:10.1246/cl.2008.1230